

# The Development of Hydrodynamically Unstable Flames

Moshe Matalon

McCormick School of Engineering and Applied Science  
Northwestern University, Evanston, IL  
matalon@northwestern.edu

Extended abstract for the 20th International Colloquium on the Dynamics of Explosions  
and Reactive Systems, McGill University, Montreal Canada

July 31 - August 5, 2005

The hydrodynamic instability, discovered independently in theoretical analyses by Darrieus [1] and Landau [2] over half a century ago, has many ramifications in combustion. The appearance of sharp folds and creases on the flame front of freely propagating flames, and the wrinkling observed over the surface of large spherically expanding flames are direct manifestations of this instability. Observations indicate that the scale of the wrinkles in such circumstances is typically much larger than the characteristic cell size of the more conventional cellular flames, which result from diffusive-thermal instabilities. Furthermore, the wrinkled flame is seen to accelerate as it propagates further and may turn into a turbulent flame when reaching a sufficiently large size. The nonlinear development of hydrodynamically unstable flames is not only important for understanding the structure and dynamics of fast enough and large-scale flames, but is also a prerequisite for the analysis of unconfined transitions to detonations.

Studies of the hydrodynamic instability and its consequences are appropriately discussed within the framework of a *hydrodynamic theory*. Accordingly, the whole flame, associated with the region where chemical reaction, diffusion, heat conduction and viscous effects take place, is assumed thin when compared to the representative length scale of the fluid flow. Consequently, the flame is represented by a sheet and the flow field on either side is determined by solving the incompressible hydrodynamic equations with different densities for the burnt and unburnt gases. By resolving the internal structure of the flame on the smaller diffusion scale, appropriate jump conditions for the pressure and velocities across the front, as well as an equation for the flame speed, are obtained as matching conditions. The resulting model is a nonlinear free-boundary problem supplemented with conditions that describe influences of the diffusion processes within the flame zone. The hydrodynamic model has been employed in analytical studies of flame front instabilities. Simple solutions of this model corresponding to plane, spherical and strained flames are easily obtained, and thus could be used as basic states in examining the evolution of small disturbances. Numerous such studies have been presented in recent years elucidating the unique characteristics of instabilities in flames, including the onset of cellular flames and other corrugated structures.

In this presentation we focus on spherically expanding flames and the associated self-wrinkling phenomenon observed in relatively large flames. Linear stability analysis in this case provides an explicit expression for the critical flame size at the instability threshold in terms of all relevant physicochemical parameters [3]. In dimensionless form, the marginal stability conditions are expressed as  $Pe = \mathcal{F}(\sigma, Le_{\text{eff}}, Pr; n)$  where  $Pe = R/l_D$  is the Peclet number representing the flame size  $R$  in units of the diffusion length  $l_D$ ,  $\sigma = \rho_u/\rho_b$  is the thermal expansion parameter (or unburnt-to-burnt density ratio),  $Le_{\text{eff}}$  is the effective Lewis number of the combustible mixture,  $Pr$  is the Prandtl number and  $n$  the spherical harmonics index. For fixed  $\sigma$  and  $Pr$ , and when the Lewis number is larger than a critical value, the marginal curves trace out a peninsula (see Fig. 1) that encompasses the range of unstable modes  $n_{\text{min}} < n < n_{\text{max}}$  as a function of  $Pe$ ; the long wavelength disturbances  $n < n_{\text{min}}$  are stabilized by stretch, and the short waves  $n > n_{\text{max}}$  by

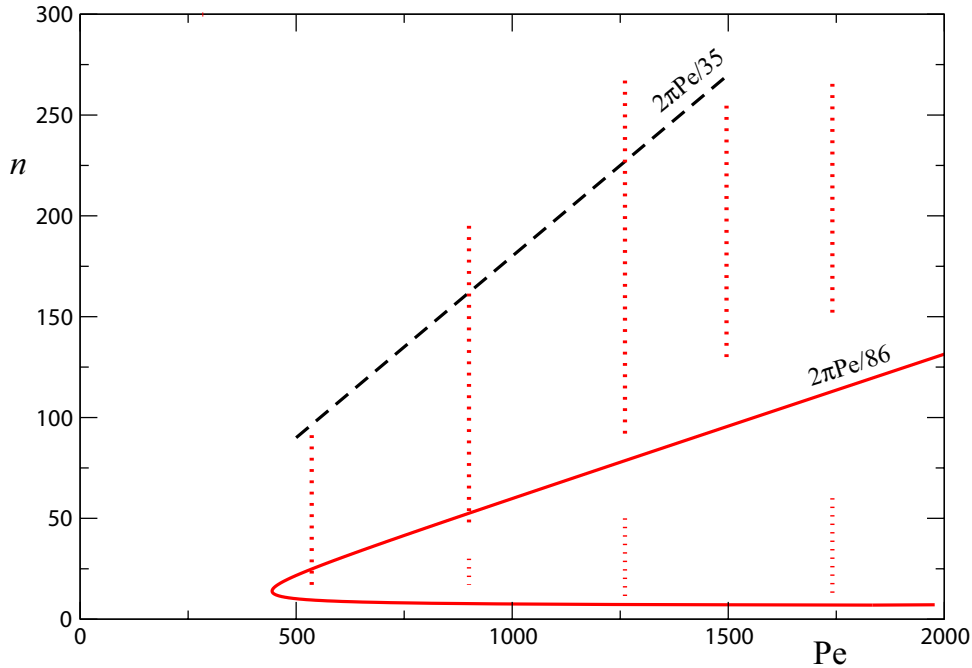


Figure 1: Marginal stability curves separating stable from unstable modes. The nose of the peninsula indicates the critical Peclet number, or radius, for the instability onset. The three curves correspond to different values of the Lewis number, shifted to the right as the Lewis number increases.

diffusion. The nose of the peninsula determines the critical radius  $R_c$  and wavelength  $\lambda = 2\pi R_c/n$  at the onset of the instability. The results may also be used to estimate the characteristic cell size observed when the flame grows further. By examining the limit of large Peclet number one finds that the largest expected cell increases with radius almost linearly, while the smallest expected cell remains nearly constant. As the flame expands, stretch is weakened and cells of larger and larger size are able to develop. When these cells reach a critical size they become unstable and new cells are formed, covering the whole flame front. Since cells that are too small cannot survive,  $\lambda = 2\pi R/n_{\max}$  may be considered a representative of the average cell size when the whole flame becomes cellular. The limiting unstable wavelengths predicted theoretically could also serve as inner and outer cutoffs in a fractal analysis, leading to an analytical expression for the developing turbulent flame speed [7],[4]. Finally, the linear theory has been recently extended to account for temperature-dependent transport coefficients [4], and radiative losses from the volume of burned gas enveloped by the flame front [5].

Using the preceding theory as the basis to interpret and correlate their observations, Bradley and coworkers [6]-[9] have experimentally investigated the development of instabilities in explosion flames. More recently Law and co-workers [10]-[12] have carried out extensive experimental studies of flame wrinkling for hydrogen/air and diverse hydrocarbon/air mixtures at atmospheric as well as elevated pressure conditions. These observations show, as predicted, that when the effective Lewis number of the mixture is sufficiently large the flame surface is initially smooth, but cells spontaneously appear on the surface once the flame reaches a critical size. In Figure 1 a marginal stability curve is plotted for conditions corresponding to the data reported in [8] for an iso-octane/air mixture, namely  $Le_{\text{eff}} = 1.65$ ,  $\beta = 7.48$ ,  $Pr = 0.7$ ,  $\sigma = 6.6$ . The calculations are based on the expressions derived in [4] allowing for variable transport with diffusivities assumed to vary with temperature as  $T^{1/2}$ . The dots in the figure are the wavenumbers recorded from a cine film of observed cells, and the dashed curve  $n_{\max} = 2\pi Pe/35$  represents the experimentally best fit of the largest unstable wavenumber. Although the prediction of the critical Peclet number compares reasonably well with the experimental data, the theory clearly overestimates the size of the smallest possible cells. This can be partially attributed to the cascade of progressively decreasing unstable wavelengths, a phenomenon occurring beyond the instability threshold and not properly accounted for in a linear theory.

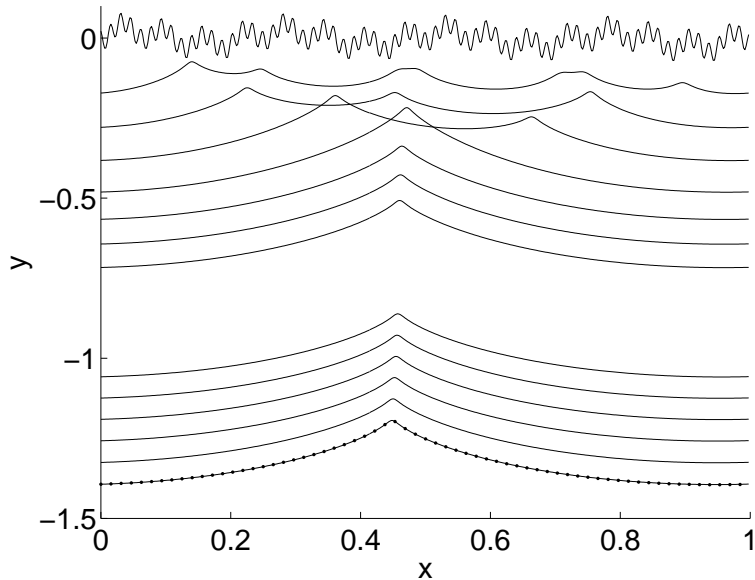


Figure 2: Development of the flame front profile based on the MS equation starting with arbitrary initial data. The disturbances introduced through the initial conditions merge, forming bigger cells which eventually coalesce into a single-peak structure that coincides with the pole-solution ( $N = 8$ ), shown in the figure as the dotted curve. Calculated for  $\alpha = 0.005$ .

Beyond the linear growth, the dynamics of a flame front must be based on the full nonlinear system of conservation laws. Since computational simulations of the complete Navier-Stokes equations for a multi-component chemically reacting mixture over sufficiently long time have met significant difficulties, progress has relied primarily on analytical and numerical investigation of simplified models. Most studies have examined the nonlinear evolution of a nominally planar front, a local approximation of a segment of a large flame. One such model is the Michelson-Sivashinsky (MS) equation obtained in the weakly-nonlinear long wave asymptotic limit. The MS model is valid when the heat release relative to the thermal energy of the fresh mixture is small, namely for values of the thermal expansion coefficient  $\sigma - 1 \ll 1$ . On a finite domain  $L$  with periodic boundary conditions the MS equation admits exact solutions, obtained by using a pole-decomposition technique, which correspond to steadily propagating cusp-like structures. Of greatest importance is the stability results [13]-[14], which show that for any value of  $L$  there exists one and only one asymptotically stable pole solution. This implies that, starting with arbitrary initial data, the long time behavior of the solution of the MS equation would always converge to the stable steadily-propagating cusp-like solution. In a typical numerical experiment, as illustrated in figure 2, the short wavelength corrugations introduced through initial disturbances merge, forming as time progresses bigger cells which eventually coalesce into a single-peak structure filling up the entire interval. The transverse coordinate  $x$  in this figure was scaled with respect to  $L$  and the flame profiles were calculated for  $\alpha \equiv \mathcal{L}/(\sigma - 1)L = 0.005$ , where  $\mathcal{L}$  the Markstein length (of the order of the flame thickness). The solution appears to converge to the corresponding pole solution ( $N = 8$ ) illustrated in the figure by the dotted curve. Thus, after a short transient, the flame develops into a relatively large single-peak structure that propagates along the negative  $y$ -axis at a constant speed. The wavelength of the corrugated front is comparable to  $L$ , i.e. much larger than the wavelength corresponding to the most amplified small disturbance predicted by the linear theory.

Although the MS equation provides valuable physical insight in the nonlinear development of the Darrieus-Landau instability, its application is limited by the fact that  $\sigma \approx 6 - 8$  for real gas mixtures. A full nonlinear model valid for realistic values of  $\sigma$  is thus necessary in order to understand the effect of thermal expansion on flame dynamics. In this presentation, we report on recent advances of flame dynamics that properly account for density variations. The computations are carried out within the context of the hydrodynamic theory. This simplified model contains fewer parameters than the full governing equations, and thus permits description of multi-dimensional

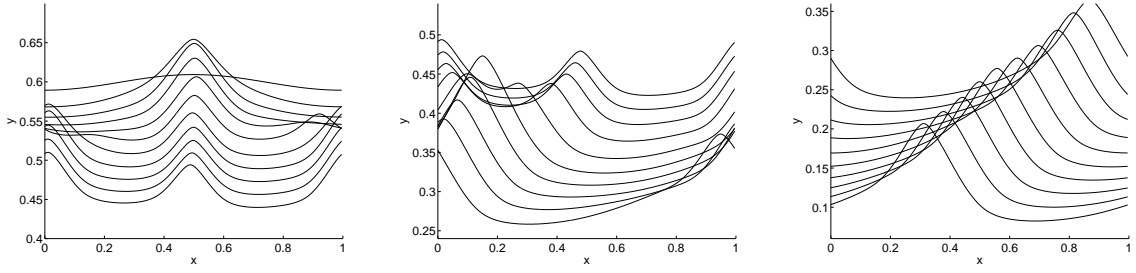


Figure 3: The time evolution of an initial cosine perturbation for  $\alpha = 0.0025$  with  $\sigma = 6$ .

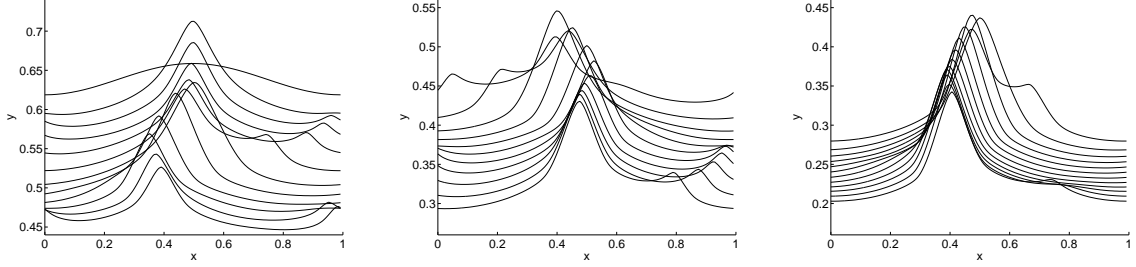


Figure 4: The time evolution of an initial cosine perturbation for  $\alpha = 0.001$  with  $\sigma = 6$ .

flames with sufficient accuracy over a wider range of conditions. Furthermore, the simulations can be carried out on a uniform grid containing a moderate number of points which reduce the computational cost significantly. As a first implementation of the numerical treatment a Markstein-type model is considered, namely a dependence of flame speed on curvature is assumed and the Rankine-Hugoniot relations are applied without modification. The numerical scheme is based on a *continuum approach* where singular sources and discontinuities are smoothed properly over several computational grid cells. The Navier-Stokes equations are solved using the variable density IAMR code, and a level set method is used as a front-capturing technique. For the advancement of the flame it is necessary to evaluate the velocity field on the Lagrangian mesh representing the flame surface and this has been accomplished using an immersed boundary method.

For illustration, the time evolution of an initial cosine perturbation is shown in figure 3 for  $\alpha = 0.0025$ , with  $\sigma = 6$ . The flame front profile is plotted at consecutive times (starting from the graph on the left and moving to the right) over a sufficiently long time interval. One finds that a smooth cusp-like structure develops and propagates at a constant speed without further change in shape. The general structure of the solution is retained in computations carried out in larger

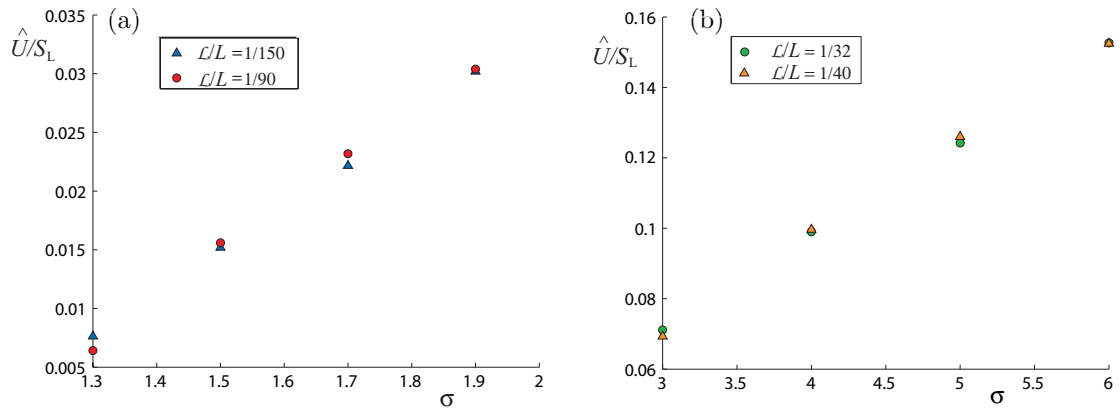


Figure 5: The dependence of the incremental increase in propagation speed  $\hat{U}/S_L$  on thermal expansion, for different values of the Markstein number  $\mathcal{L}/L$ .

domains (smaller  $\alpha$ ), except that now small wrinkles appear repetitively on the flame front, and the solution does not settle to a steadily propagating state. This is illustrated in figure 4 for  $\alpha = 0.001$ . It has been tempting to associate this peculiar behavior with a secondary-instability that occurs at a critical value of  $\alpha$ , but this assertion is inconsistent with the stability of the pole solutions. The unsteady structure in the numerical simulation seem to be an acute sensitivity to numerical noise. A low level of permanent noise provides small disturbances which are rapidly magnified by the hydrodynamic instability, resulting in small-scale wrinkles that appear sporadically on the flame, propagate along its surface, and disappear at the crests. External noise may result, for example, from a weakly turbulent flow of relatively large scale. Since the turbulent flow in such a case does not affect the internal flame structure, the flame may be viewed as a surface of density discontinuity, well within the realm of the present model. Further evidence of this conjecture will be given in the oral presentation.

Although the flame profiles appear qualitatively similar to the predictions of the MS equation, the evolving structures for realistic values of  $\sigma$  have larger amplitudes and propagate significantly faster, as shown in Figure 5. The figure shows the dependence of the incremental increase in propagation speed on thermal expansion for two values of the Markstein number  $\mathcal{L}/L$ . The ordinate in this figure represents the increment in speed  $\hat{U}$  in units of the laminar flame speed  $S_L$ , so that the corrugated front propagates as a whole in the negative  $y$ -direction with a speed  $S_L + \hat{U}$ . We see that for realistic values of thermal expansion the maximum incremental increase in propagation speed may be as large as 15% to 20%.

## References

- [1] DARRIEUS, G. 1938 Propagation d'un front de flamme. *Unpublished work*, presented at La Technique Moderne (Paris), and in 1945 at Congrès de Mécanique Appliquée (Paris).
- [2] LANDAU, L.D. 1944 On the theory of slow combustion. *Acta Physicochimica USSR* **19**, 77.
- [3] BECHTOLD J.K., AND MATALON, M., 1987 Hydrodynamic and Diffusion Effects on the Stability of Spherically Expanding Flames, *Combust. Flame*, **67**, 77
- [4] ADDABBO R. BECHTOLD J.K. AND MATALON M. 2002 Wrinkling of Spherically Expanding Flames *Proc. Combust. Inst.* **29**, 1527–1535
- [5] BECHTOLD J.K., CUI C. AND MATALON M. 2005 The Role of Radiative Losses in Self-extinguishing and Self-wrinkling Flames *Proc. Combust. Inst.* **30**, 177–184.
- [6] BRADLEY, D. & HARPER, C.M. 1994 The development of instabilities in laminar explosion flames. *Combust. Flame* **99**: 562-573
- [7] BRADLEY, D. 1999 Instabilities and flame speed in large-scale premixed gaseous explosions. *Phil. Trans. R. Soc. London, A.* **357**, 3567–3581.
- [8] BRADLEY D. SHEPPARD C.G.W. WOOLLEY R., GREENHALGH D.A. AND LOCKETT R.D., 2000 The Development and Structure of Flame Instabilities and Cellularity at Low Markstein Numbers in Explosions, *Combust. Flame*, **122**, 195
- [9] BRADLEY, D., CRESSWELL, T.M. AND PUTTOCK, J.S. 2001 Flame acceleration due to flame-induced instabilities in large-scale explosions. *Combust. and Flame* **124**, 551–559.
- [10] TSE, S.D., ZHU, D.L. AND LAW, C.K. 2000 Morphology and burning fluxes of expanding spherical flames in H<sub>2</sub>/O<sub>2</sub>/inert mixtures up to 60 atmospheres *Proc. Combust. Inst.* **28**, 1793–1800.
- [11] KWON, O.C., ROZENCHAN, G. AND LAW, C.K. 2002 Cellular instabilities and self-acceleration of outwardly propagating spherical flames *Proc. Combust. Inst.* **29**, 1775–1783.
- [12] LAW, C.K. 2005 Propagation, Structure, and Limit Phenomena of Laminar Flames at Elevated Pressures, submitted for publication.
- [13] VAYNBLAT, D. & MATALON, M. 2000a Stability of pole solutions for planar propagating flames: I. Exact eigenvalues and eigenfunctions. *SIAM J. Appl. Math.* **60**, 679–702.
- [14] VAYNBLAT, D. & MATALON, M. 2000b Stability of pole solutions for planar propagating flames: II. Properties of eigenvalues/eigenfunctions. *SIAM J. Appl. Math.* **60**, 702–728.